ISSN 8755-6839

SCIENCE OF **TSUNAMI HAZARDS**

Journal of Tsunami Society International

Volume 41 **Number 3** **2022**

POSSIBLE TSUNAMIS IN THE ARCTIC

Mazova R. Kh., Kurkin A.A., Vinokurov M.S.

Nizhny Novgorod State Technical University n.a. R.E. Alekseev. Russia.
e-mail: *raissamazova@yandex.ru*

ABSTRACT

The Arctic is the least studied region in terms of problems associated with earthquake and tsunami phenomena. Usually, the tsunami hazard in the Arctic is considered insignificant. This is primarily due to the low seismic activity of the region. In connection with the economic development of the shelf, the problem of tsunami hazard on the Arctic coast becomes to be actual and requires detailed studies of the probable events of tsunami wave generation. This present study considers the potential problem of the tsunami hazard in the Arctic region, and provides estimates of possible tsunami wave heights on the shelves of the Arctic coasts of the Baffin Sea, the Laptev Sea and the Beaufort Sea. On the basis of the keyboard model of the subduction zone, a number of scenarios of the possible occurrence of earthquakes with source in the area of localization of historical source of the earthquake in 1933, (M=7.7, 1964, M=6.7, 1920, M=6.4) were considered.

Key words: *Arctic Ocean, Arctic shelf, earthquake key-board model, tsunami, numerical simulation.*

1. INTRODUCTION

Presently, one of the main priorities is the Arctic Ocean region. Moreover, its geopolitical role and mainly its economic role is increasing globally. The Arctic region has a unique strategic hydrocarbon resource potential. Long-term interests of a large number of nations of the world are associated with the Arctic region. The territories of the Arctic include the northern part of the Earth, which includes five subarctic states. These are: Russia, Canada, the United States of America, Norway and Denmark. In general, today the northern regions are acquiring new significance in connection with the development of world economic ties. Questions of development of Arctic oil and gas resources are relevant due to the strategic importance of hydrocarbons [1-6].

It is well known that most earthquake epicenters are confined to tectonically active faults. In accordance with the classical picture of the division of the lithosphere into plates, the boundary between the North American and Eurasian plates runs along the mid-ocean ridge, stretching from Iceland through the Norwegian-Greenland basin and the Gakkel ridge in the Eurasian basin, and then abuts against the continental shelf of the Laptev Sea. In the Arctic region, modern tectonic processes in the Earth's crust are poorly understood, since stresses and strains in fault zones change rapidly as a result of tectonic movements [5,6,9-11]. For example, the seismicity of the shelf in the water area of the Laptev Sea is well known, but there is little data on the manifestation of past and present-day bottom crustal movements. Nothing much is known about crustal deformations and the possibly weak seismicity on the shelf of the East Siberian Sea. Due to insufficient information on the seismicity of the Arctic region, earthquakes and the possibility of tsunami generation are one of the main causes of man-made accidents in the development of the shelf. This is especially connected with the prospect of the extraction of hydrocarbon resources on the shelf, which are also vulnerable to potential landslides.

In connection with the intensive development of the natural resources of the Arctic, the analysis of the possible occurrence of tsunami waves on the shelves of the Arctic region is one of the priorities for the development of science. Since such natural phenomena as tsunamis have not been adequately studied in the Arctic region, the only possibility for assessing the tsunami hazard on the coasts of this region is by numerical modeling of a possible tsunami occurrences in areas with high tectonic activity, such as in the Lappet Sea [4-6,8,12]. A number of studies completed thus far indicate that tsunami waves in the Arctic can reach as much as 4-5 meters in height. On the Russian side of the shelf, wave heights have been small - up to 1 meter - but with an increase in wave activity, a trend is observed, indicating that these heights can be significantly higher [3,4,6,8]. Studies on the tsunami hazard on the coast of Canada [8,9,11], examined two zones of potential hazard on the Arctic coast: the Baffin Sea and the mouth of the Mackenzie River in the Beaufort Sea [10, 12]. Destructive waves at these two zones can also be generated by local effects such as landslides and icebergs but also by meteorites [5,6,7].

Estimates of potential tsunami wave generation by earthquakes and landslides on the Arctic shelves will result in better planning for the extraction of hydrocarbon resources on the shelf, as well as for the most relevant organization of marine activities. As presented in [9], the first instrumental information about earthquakes in the Arctic was obtained in the beginning of the 20th century and was

based mainly on data from remote seismic stations. Basically, only events with magnitude M>5.5 were recorded in the Arctic. Figure 1 [3,8] shows the epicenters of the strongest earthquakes in the Arctic Ocean basin and in adjacent territories. It is clearly seen from this map that the strongest earthquakes in coastal areas, and the more likely to generate tsunamis, can occur in the Baffin, the Greenland, the Laptev, and the Beaufort Seas. These earthquakes in these seas had magnitudes of M>6. As a rule, smaller magnitude earthquakes with sources located far from the coasts, cannot generate tsunamis that can cause significant damage to the coastal infrastructures.

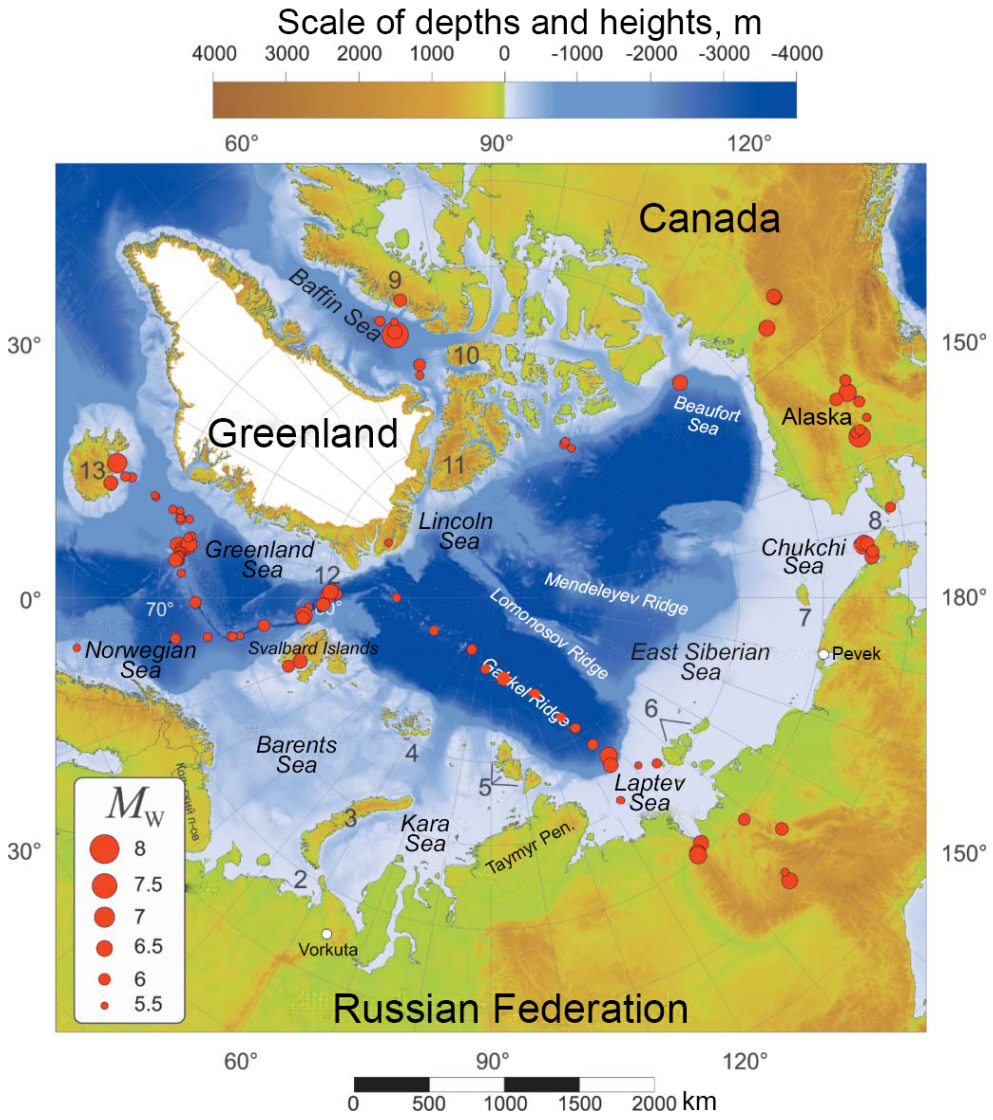

Fig.1. Epicenters of the strongest earthquakes in the Arctic Ocean basin and nearest areas (to the north from latitude 65°N) with magnitude Mw ≥ 5.5 for the period of instrumental seismological observations 1918-2011. [3,8]

2. PROBLEM STATEMENT

The present study considers areas of the Arctic waters where historical earthquakes with a magnitude of $M > 5.5$ were recorded, in some cases accompanied by tsunami waves. Earthquakes were considered in the Baffin Sea on November 20, 1933, $M = 7.7$, in the Laptev Sea on May 30, 1923, $M = 6.7$, on May 30, 23, $M = 6.0$, on April 7, 1969, $M = 5.5$, and in the Beaufort Sea on November 16, 1920, M=6.4 [8-12].

In contrast to the numerical simulation of these events considered in [8], in the proposed work, the dynamics of a seismic source is considered within the framework of a block-keyboard model of a seismic source [13]. The computational area used for modeling in the Baffin Sea is [-79.62^0 - 60.23^0 (E), 79.67^0 - 64.57^0 (N)]. In the water area of the Laptev Sea, the area [-79.62^0 -60.23^0 (E), 79.67^0 - 64.57^0 (N)] was used; for the Beaufort Sea, the area [121.29^0 -140.23^0(E), 69.92^0 -79.50^0(N)] was considered.

The simulation was carried out on a grid with a space step of 1 min and a time step of 1 s. Since, as noted above, there is little data on the manifestation of modern bottom movements in the Arctic region, the modeling was carried out on the basis of a keyboard- block- model of an earthquake, which allows us to consider different implementation of the dynamics of the earth's crust in the area of a seismic source for a given earthquake magnitude (see., e.g., [16, 18,19]). For this purpose, 2- and 3-block seismic sources were formed for the Baffin Sea, a 4-block seismic source for the Laptev Sea, and a two-block seismic source was considered for tsunami modeling in the Beaufort Sea.

The length and width of the rupture in the earthquake source was determined using the Lamb formulas for earthquake magnitudes for these events [15], and the maximum displacement of the wave surface above the earthquake source was determined using the Iida formula [16], (see.1a,b)

$$\lg L = 0.5M - 2{,}44 \pm 0{,}16 \qquad (1a)$$

$$\lg W = 0.32M - 1.01 \pm 0.15$$
$$\lg H = 0.8M - 5{,}6 \qquad (1b)$$

3. NUMERICAL SIMULATION OF TSUNAMI WAVES FROM THE 20 NOVEMBER 1933 BAFFIN SEA EARTHQUAKE

Numerical simulation was carried out within the framework of nonlinear shallow water equations (see., e.g., [17-20]). For numerical simulation of the processes of generation and propagation of waves in a two-dimensional formulation, the Sielecki scheme [21] was chosen. Two scenarios of generation of a tsunami source by a seismic source were considered in the work: Scenario 1 - two-block model; Scenario 2 - three-block model. Approximate dimensions of the outbreak were: 130 km x 30 km. The localization of the earthquake source is shown in fig. 2 and 3. Red dots and numbers mark the location of virtual tide gauges. Red squares highlight the area of localization of the focus.

Scenario 1.

Figure 2 shows the localization of a two-block earthquake source for this scenario. The epicenter of the earthquake is located in the first block, oriented towards the coast of Greenland. Table 1 shows the kinematics of blocks in the earthquake source. The movement of blocks starts from block 1, down by 4m, after 20 seconds the second block starts moving up by 7. m.

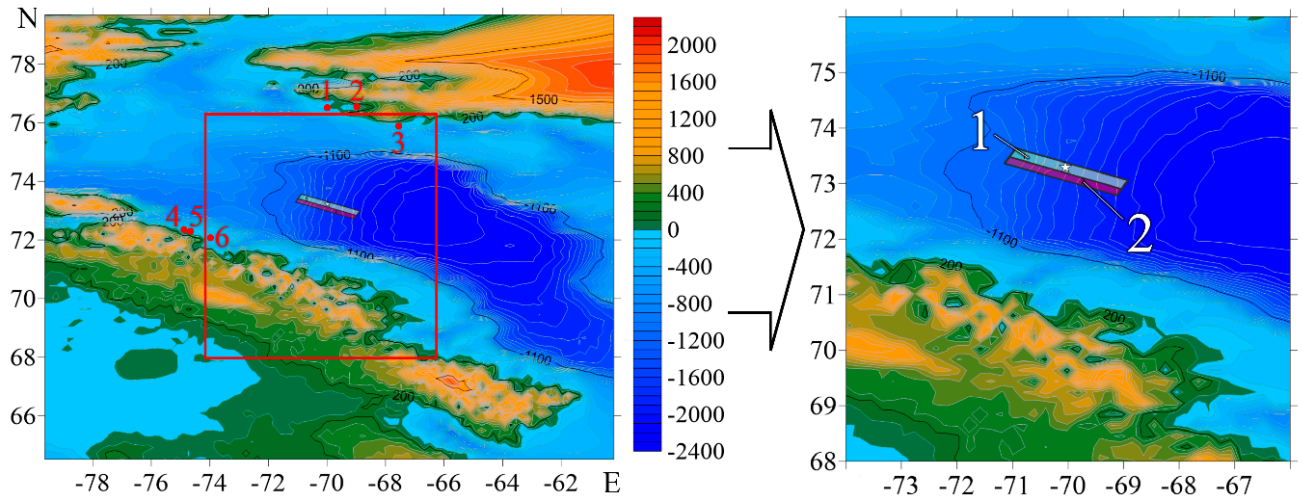

Fig. 2. Earthquake source location in the Baffin Sea (Scenario 1)

Table 1. Kinematics of block motion in the earthquake source (Scenario 1)

Scenario 1		
Block movement	**Block 1**	**Block 2**
Height (m)	**6**	**-4**
Start time of movement (s)	**0**	**0**
Final time of movement (s)	**60**	**20**

Fig.15 shows the picture of wave front propagation in the Beaufort Sea for 6 time moments. in Fig.15 (1)(2) it can be seen wave front position in the initial time moments. In Fig.15 (3) it is seen the approaching the wave front to Banks Island and the approach of the wave to the mouth

Scenario 2.

In this scenario, a three-block source was considered, with the same dimensions and the same magnitude of the earthquake. The epicenter of the earthquake is located in the first block. Figure 3 shows the localization of the earthquake source for Scenario 2 in the calculated water area.

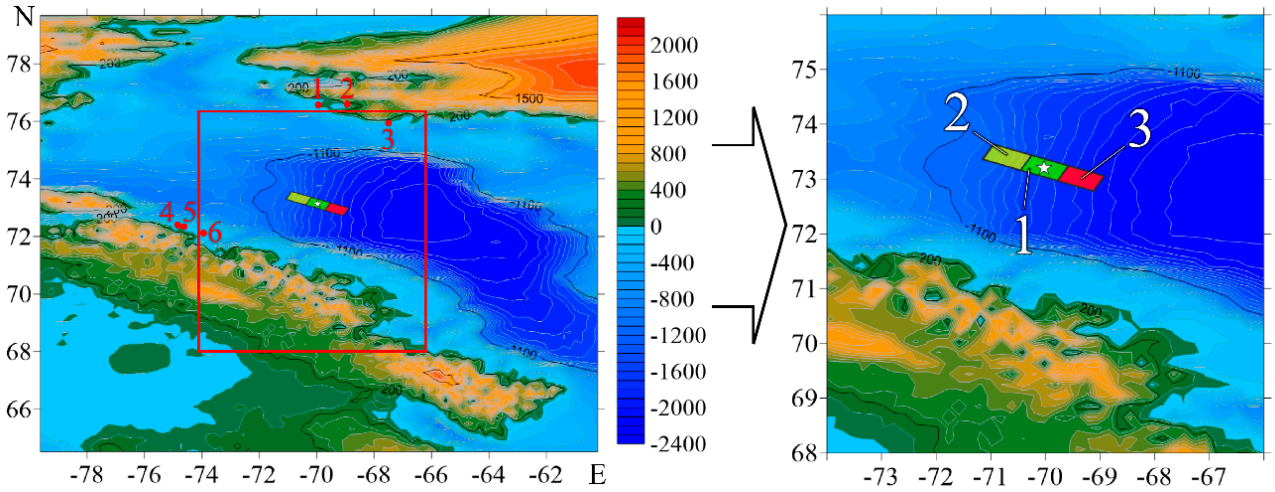

Fig. 3. Earthquake source location in the Baffin Sea (Scenario 2)

The kinematics of the movement of the blocks is presented in Table 2. The beginnings of the movement of each block were implemented at different times.

Table 2. Kinematics of blocks motion in the earthquake source (Scenario 2)

Scenario 2			
Block movement	**Block 1**	**Block 2**	**Block 3**
Height (m)	**6**	**-4**	**4**
Start time of movement (s)	**0**	**20**	**50**
Final time of movement (s)	**30**	**50**	**105**

For Scenario 1, Fig. 4 shows the generation of the tsunami source for 1 minute when the key-blocks move in the earthquake source (see Table 1), and the further propagation of tsunami waves over the water area.

For scenario 2, Fig. 5 shows the generation of the tsunami source for 105 sec when the keyblocks move in the earthquake source (see Table 2). It is clearly seen that the tsunami source is formed as the blocks move in the earthquake source. Figure 6 shows the propagation of wave fronts for two moments of time. The computation results show that in almost an hour the wave front reaches the coast of Greenland and then propagates along it. Figure 7 shows the distribution of maximum wave

heights over the computed water area for both scenarios. It is clearly seen that for the first scenario, large wave heights off the coast of Nunavut. Near Round Island, wave heights are about 10 meters. Off the coast of Greenland, near the village of Pituffik, the wave heights are about 0.3m. However, when approaching Melville Bay, the heights of the waves grew sharply. Waves do not exceed 1 meter off Wolstenholme Island. On Bylot Island, in some areas, the wave height reached 3 meters, the average heights on the coast were much lower.

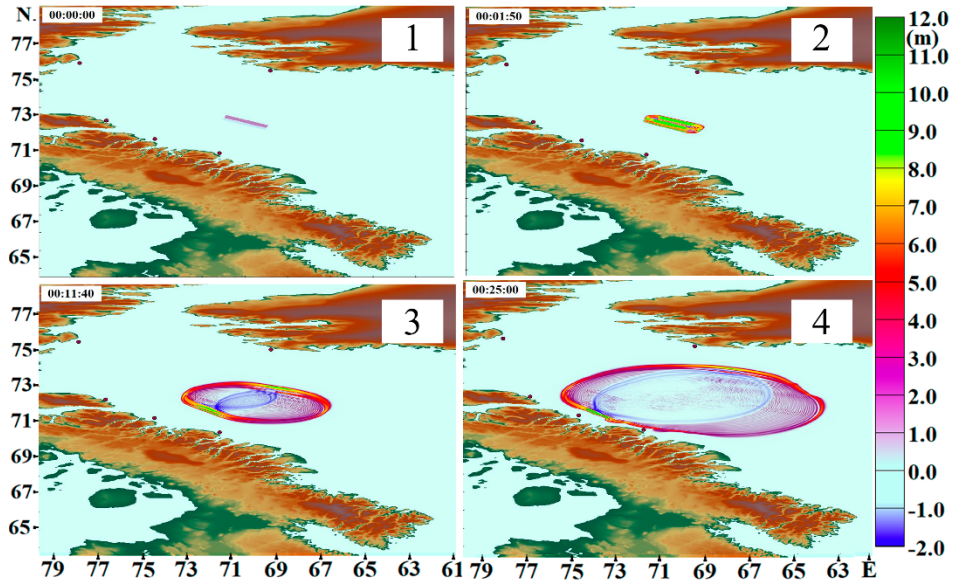

Fig. 4. Time moments of tsunami wave generation and propagation in the Baffin Sea: generation of the tsunami source and 3 moments of wave propagation time across the water area (Scenario 1)

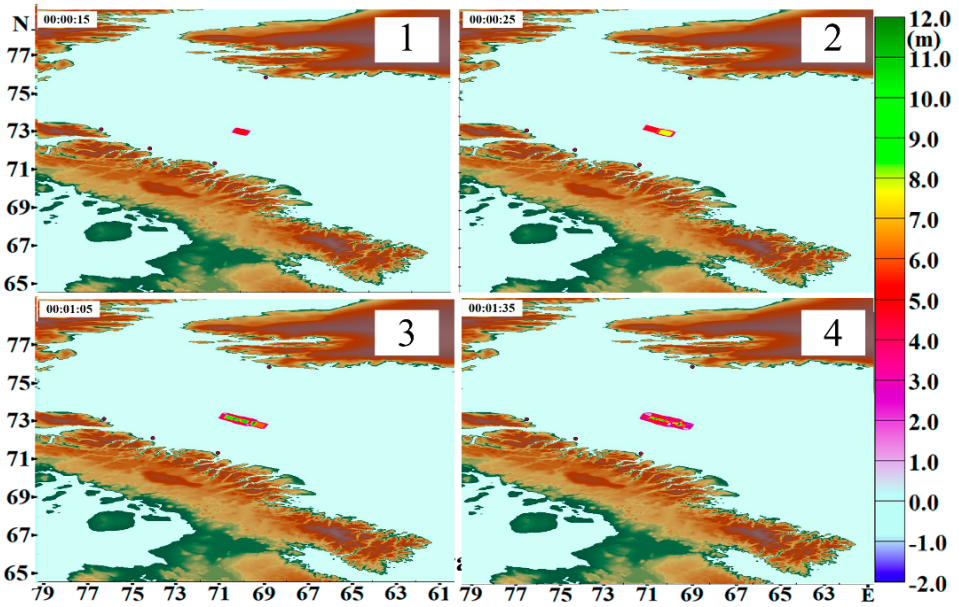

Fig. 5. Tsunami wave generation in the Baffin Sea (Scenario 2)

For the second scenario, wave heights off the coast of Nunavut, near Round Island, are significantly lower, but exceed 5 meters.

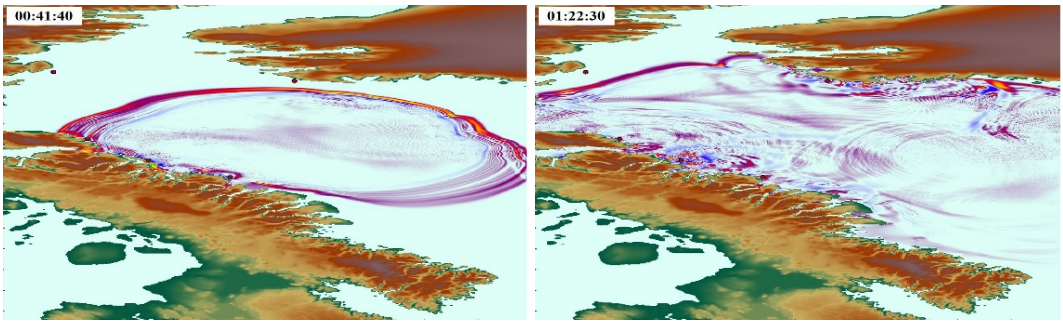

Fig. 6. Two time moments of the wave propagation in the Baffin Sea (Scenario 2).

Off the coast of Greenland, near the village of Pituffik, wave heights are about 0.5m. Near Melville Bay, waves reach heights of up to 5m. The average wave height on the coast is in the range of 2-3m. Unlike the first scenario, there is no sharp increase in wave height near the Round and Nova Zembolla islands, the waves do not exceed 5 meters.

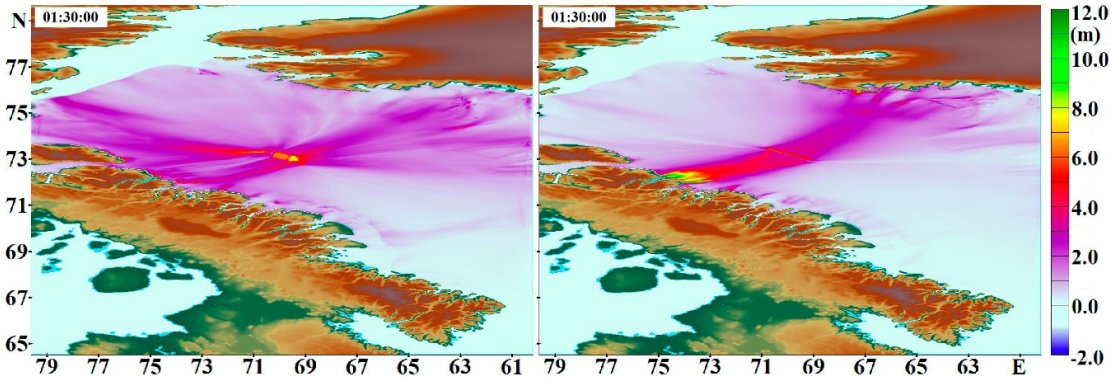

Fig. 7. Distribution of maximum wave heights in the computation area of the Baffin Sea for: a) two-block source (Scenario 1); c) three-block source (Scenario 2)

On Bylot Island, the height also fluctuates around 5m. This is clearly seen in the histograms shown in Fig. 8 and Fig. 9, and the average wave height was about 2 meters. The height of the waves on the coast of Greenland fluctuates on average at around 2 meters. A small surge in wave height is seen near Melville Bay, similar to Scenario 1, but in this case only up to four meters. On the histograms for Scenario 1 (Fig. 8a), one can see that on Bylot Island, the wave height reaches three meters in some parts of the coast, closer to Round Island. The average wave height is 1.5 meters. The wave height on the coast of Greenland is much higher, which is clearly seen in Fig. 8b. A sharp rise in height is seen near Melville Bay, with waves reaching over 8 meters in height. The average wave height off the coast of Greenland does not exceed four meters.

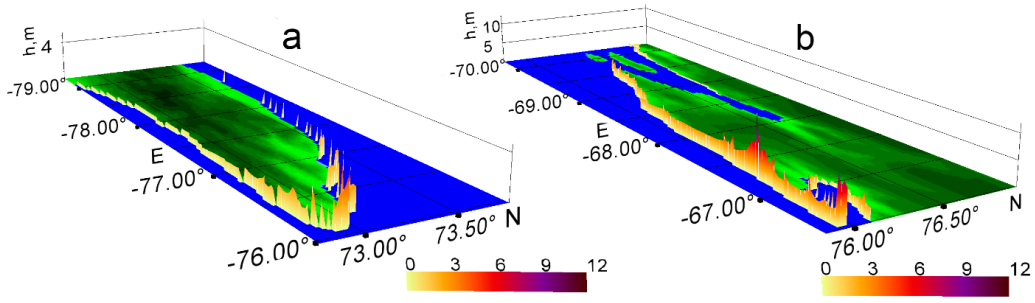

Fig. 8 3D histograms of the distribution of maximum wave heights on: a) Baylot Island; b) Greenland coast (Scenario 1)

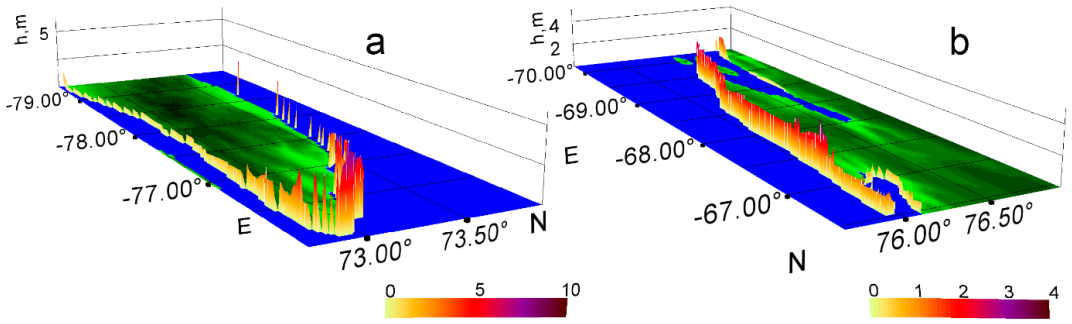

Fig. 9 3D histograms of the maximum wave height distribution on: a) Baylot Island; b) Greenland coast (Scenario 2).

Figure 9. shows histograms for Scenario 2. It is well seen that wave heights along overall coast are essentially lower as compared with scenario 1. The data from 6 virtual tide gauges (Fig.2, Fig.3) in different parts of the Baffin Sea for both scenarios are presented in Table.3.

Table 3. Data on maximum wave displacement at 5 m isobath (according to tide gauge data) for Scenario 1 and Scenario 2

Point	Maximum height	
	Scenario 1	Scenario 2
(1) Wolstenholme Island, Greenland	**0,53**	**0,81**
(2) Pituffik, Greenland	**0,30**	**0,26**
(3) Melville Bay, Greenland	**2,14**	**1,08**
(4) Nova Zembla Island, Canada	**5,27**	**2,43**
(5) Round Island, Canada	**7,76**	**2,15**
(6) Davis Strait, Canada	**5,88**	**3,83**

It is clearly seen that with different implementation of the movement of key-blocks in the seismic source for the same earthquake magnitude, the possible implementation of wave heights on the coast can be significantly different. This indicates the need to take into account additional factors, such as geostructures, detailed bathymetry, and coseismic displacements.

4. NUMERICAL SIMULATION OF TSUNAMI WAVE GENERATION AND PROPAGATION IN THE LAPTEV SEA - Tsunami source formation for the Laptev Sea.

A generalized source was formed in the Laptev Sea, which included three earthquakes: 1923, 1964 and 1969. The source was divided into 4 blocks, their movements and sizes were corrected for earthquakes of the corresponding magnitude. A generalized source was formed in the Laptev Sea, which included three earthquakes: 1923, 1964 and 1969. The source was divided into 4 blocks, their movements and sizes were corrected for earthquakes of the corresponding magnitude.

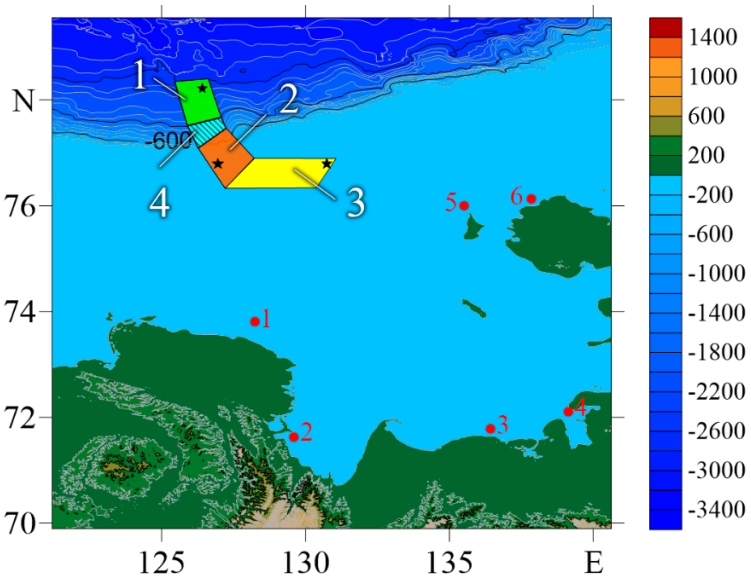

Fig. 10. Computation water area and earthquake source of the scenario in the Laptev Sea. Location of blocks (1,2,3,4) and virtual tide gauges in the scenario (red figures): 1 – coastal area of the Lena Reserve; 2 - Tiksi; 3 - Nizhneyansk; 4 - Yukagir; 5 - 6 near Belkovsky and Kotelny islands, respectively.

Figure 10 shows the location of the blocks in the calculated water area. The first one corresponds to the earthquake of 08/25/1964 with M=6.7, the localization of the second block corresponds to the earthquake of 05/30/1923 with M=6.0, the third block is located to the east of the second block and approximately corresponds to the earthquake of 04/07/1969 with M=5.5. The last, fourth block is formed between the first and fourth blocks, as an area of a possible earthquake. The shapes of the blocks are somewhat distorted due to the modeling in the Cartesian coordinate system.

Table 4 shows the kinematics of block motion in the source, based on a number of data from [6–9]. The first block moves up for 30 seconds to a height of 2m. The second block starts its downward movement 15 seconds after the start of the movement of the first block and moves for 15 seconds, the displacement is -1.5 m, and the third and fourth begin their movement after 10 and 20 seconds, respectively, and move for 15 and 10 seconds, with a positive displacement of 1, 8m and -1m.

Table. 4. Kinematics of blocks in the seismic source.

Scenario for a generalized seismic source				
Block movement	**Block 1 25.08.1964 M=6.7**	**Block 2 30.05.1923 M=6.0**	**Block 3 07.04.1969 M=5.5**	**Block 4**
Height (m)	**2,6**	**-1,5**	**2**	**-1,0**
Start time of movement (s)	**0**	**15**	**10**	**20**
Final time of movement (s)	**30**	**30**	**35**	**40**

4A. Numerical simulation results in the Laptev Sea

Figure 11 shows the results of numerical simulation of the generation of a model tsunami source during an earthquake in the Laptev Sea. At the moment of time 10 (Fig. 11.1) seconds, the tsunami center begins to form during the movement of the first block. The beginning of the formation of the tsunami source above block 2 can be seen in Fig. 11(2). By the 20th second, all blocks began to move, which is clearly seen from the formation of the tsunami source in Fig. 11(3). The completion of the generation of the tsunami source during the considered seismic process can be seen in Fig. 11(4).

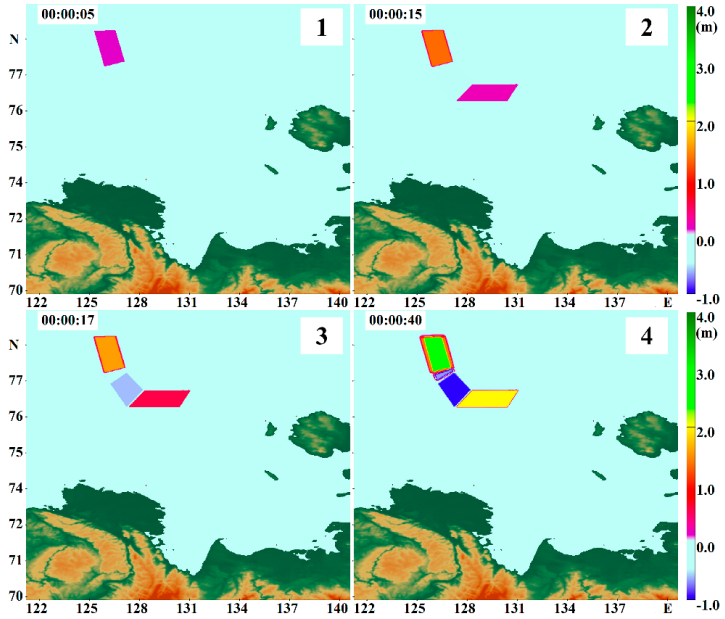

Fig. 11 Generation of the tsunami source by a four-block seismic source in the Laptev Sea.

Figure 12 (1-4) shows the formation of a wave front approaching Kotelny Island. In Fig.12(5). It is clearly seen that the wave front reaches the coast of Kotelny Island, the wave height at a given time (4 hours, 30 minutes) does not exceed one meter. In Fig. 12.6, the waves continue their propagation towards the continent.

Figure 13 shows 3D histograms: Figure 13a is a histogram of Kotelny Island from the southern side of the island. The maximum height on the histogram is just over two meters. The average height on the south side is about two meters. On the eastern side, the average wave height does not exceed one meter. Figure 13b shows the histogram of the Lensky Reserve, the maximum wave height does not exceed 1.3 meters. The average wave height is about 0.7 meters. The height of the waves to the east coast decreases. The maximum wave height reaches half a meter near the settlement of Nizhneyansk, in this area the highest wave height was recorded. On average, the wave height east of the Lensky Reserve did not exceed 0.3 meters.

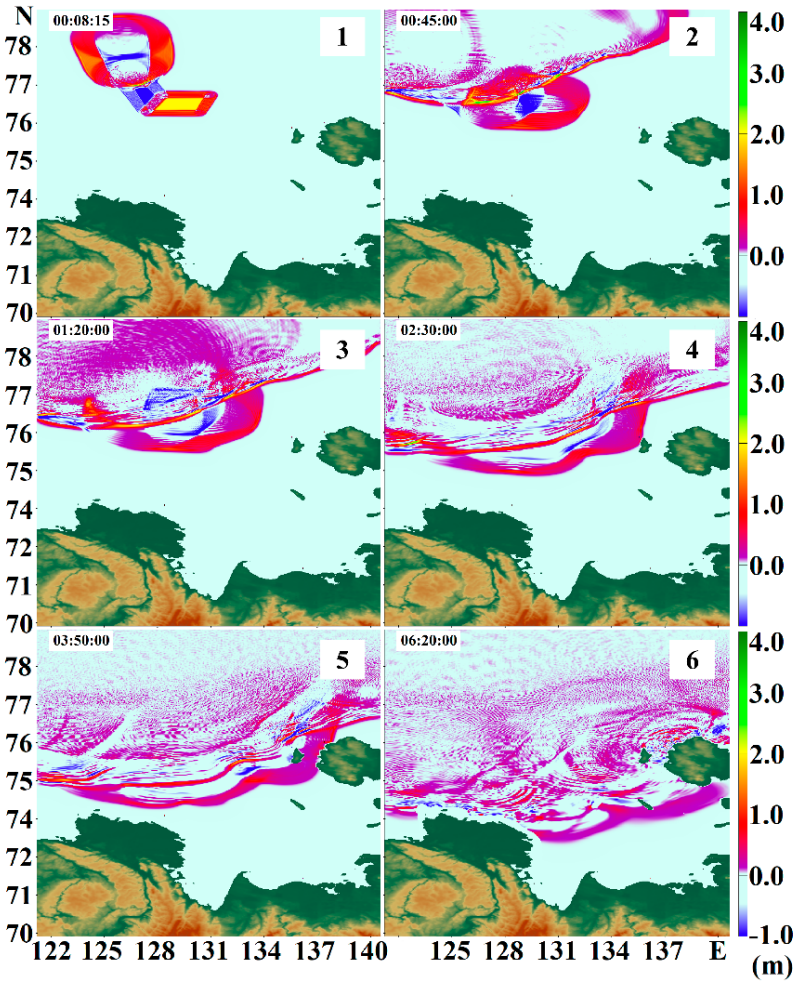

Fig. 12 Propagation of the wave fronts from the tsunami source in the Laptev Sea for 6 times moments.

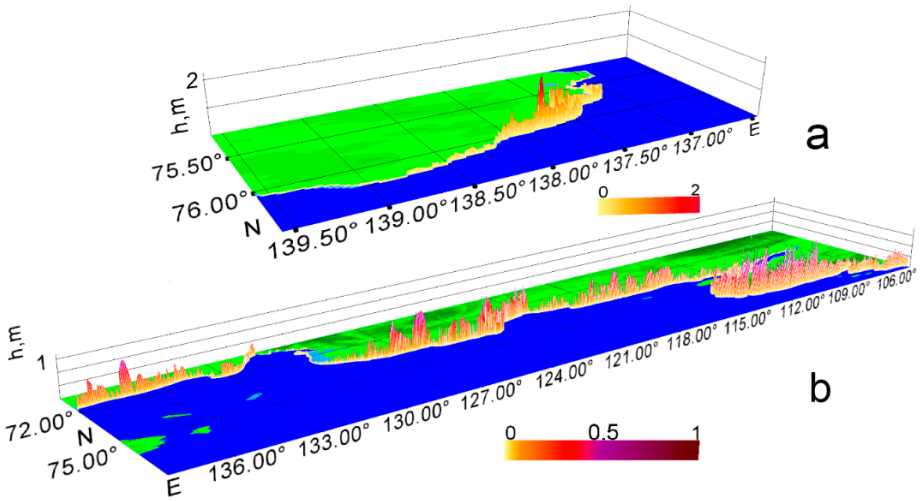

Fig.13. 3D histogram of the maximum wave height distribution : (a) along the coast of Kotel Island; (b) along the entire coast of the computation water area. Kotelny.

The data from 6 tide gauges (see Fig.10) are presented in Table 5.

Table 5. Data on maximum and minimum heights of wave displacement on the 5-meter isobath (according to tide gauge data) in the Laptev Sea

Point	Max. height, m	Min. height, m	Time, s
(1) Belkovsky Island, Russia	**0.53**	**-0.68**	**2:42:05**
(2) Kotelny Island, Russia	**1.29**	**-2.13**	**3:49:35**
(3) Nizhneyansk, Russia	**0.29**	**-0.36**	**9:34:10**
(4) Lensky Reserve, Russia	**0.39**	**-0.71**	**4:04:10**
(5) Tiksi, Russia	**0.09**	**-0.08**	**10:19:35**
(6) Yukagir, Russia	**0.26**	**-0.36**	**10:08:45**

It is clearly seen that at given magnitudes of earthquakes, the maximum wave heights near the continental and island coasts of the Laptev Sea do not exceed 1.3 m. The average wave height on the 5-meter isobath is about half a meter.

5. NUMERICAL SIMULATION OF TSUNAMI GENERATION AND PROPAGATION IN THE BEAUFORT SEA

The historical event that occurred on November 16, 1920 with a magnitude M=6.4 to the west of about. Banks is considered. Earthquake epicenter coordinates: -131.67 W (E), 72.638 N (N). To

simulate the generation of tsunami waves in the calculated water area of the Beaufort Sea, by a seismic source (Fig. 14), the localization of the earthquake source was chosen in such a way that the epicenter is located in the first block, the second block is located closer to the coast of the island. Banks. The red numbers indicate the localization of virtual tide gauges. The red square marks the localization area of the earthquake source.

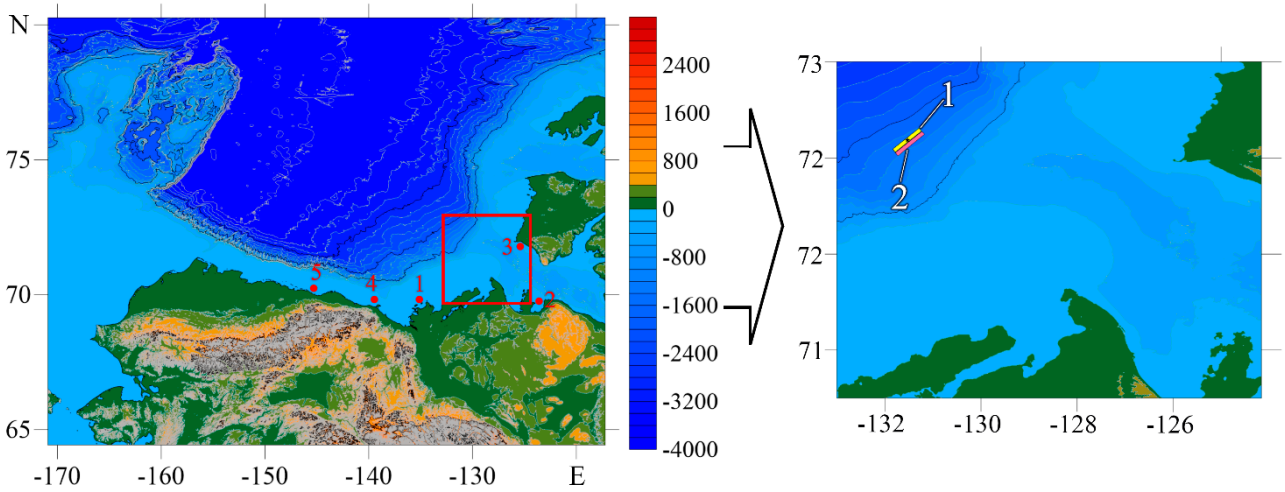

Fig. 14. Earthquake source location in the Beaufort Sea

Table 6 shows the magnitude of the displacement of the first and second blocks, as well as the times during which these displacements occurred. The size of the source, calculated according to the Wells formulas, was approximately 32x15 km. The displacement of the water surface above the earthquake source, found by the Iida formula, was about 3m. Block 1 starts moving up 3m in 30 seconds, after 10 seconds block 2 starts moving down 2.5m in 20 seconds. Thus, the generation of the tsunami source ends 30 sec after the blocks start moving in the earthquake source.

Table 6. Kinematics of blocks in the seismic source in the Beaufort Sea

Scenario for a generalized seismic source		
Block movement	**Block 1**	**Block 2**
Height (m)	**3**	**-2,5**
Start time of movement (s)	**0**	**10**
Final time of movement (s)	**30**	**30**

Fig.15 shows the picture of wave front propagation in the Beaufort Sea for 6 time moments/ in Fig.15 (1)(2) it can be seen wave front position in the initial time moments. In Fig.15 (3) it is seen the approaching the wave front to Banks Island and the approach of the wave to the mouth

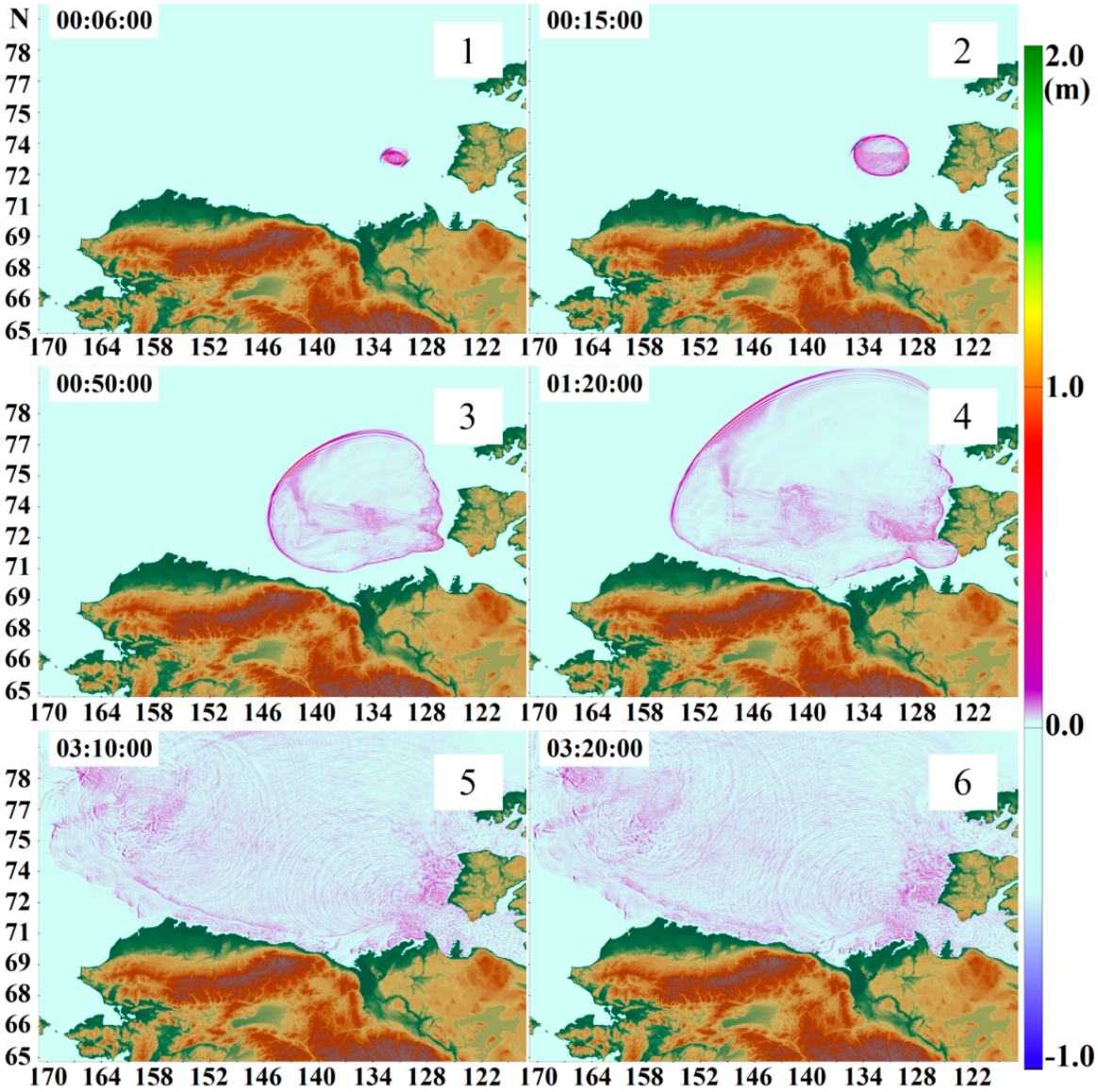

Fig. 15. Tsunami wave propagation in the Beaufort Sea for the scenario considered.

between the island and the continent. At the time point of 1 hour and 20 minutes (Fig. 15 (4)) the waves reach the Banks Islands and approach the coast of Canada. On fig. 15(5) and (6) it can be seen that the wave fronts reach the nearest parts of the coast. Thus, 3 hours and 30 minutes passed from the moment of wave generation to its approach to land. The distribution of maximum wave heights over the calculated water area is shown in Fig.16. After the movement of blocks in the earthquake source and the end of the generation of the tsunami source, the wave height rapidly decreases, and it is clearly seen that the approaching waves to the Banks Islands do not exceed 1.5 meters. According to fig. 16 and 17 you can see that the highest waves are possible on the western part of the Banks Islands.

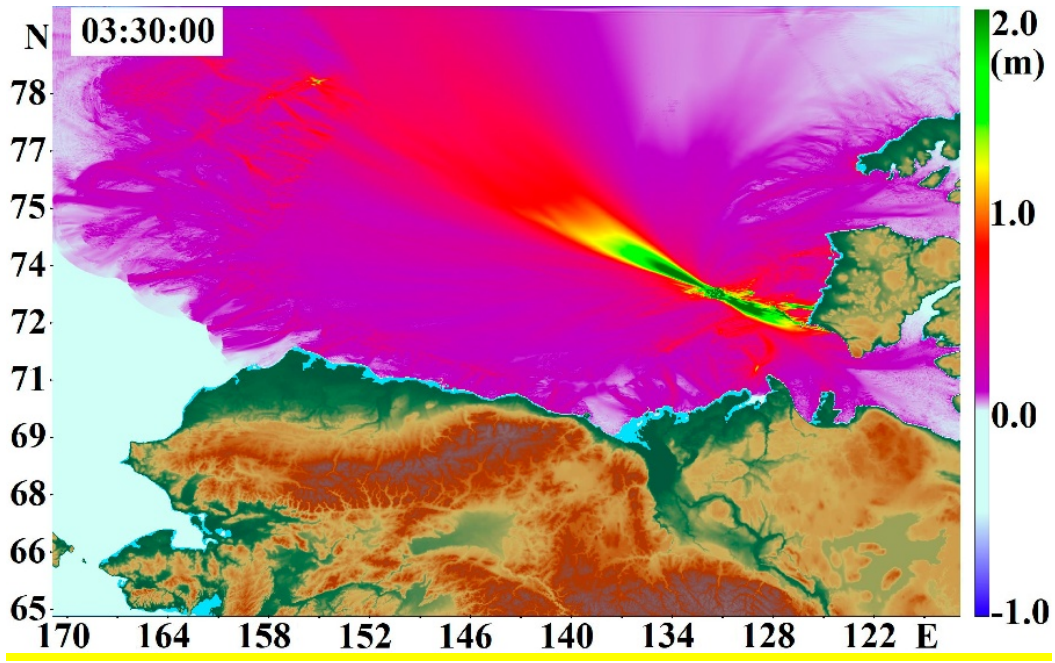

Fig. 16. Maximum wave heights in the Beaufort Sea water area in the studied scenario.

Waves of the order of one meter can be seen next to Sachs Harbour. Waves approaching the settlement of Tuktoyaktuk do not exceed 0.5 meters, and along numerous reserves in the southern direction, wave heights occasionally approach 0.5 meters, reaching an average of 0.3 meters. On the histogram in Fig. 17, it is clearly seen that the maximum wave heights are slightly more than 1 meter. The average wave height is about half a meter on the entire western coast of the island. Rare peaks of wave heights can be explained by bays and places of river mouths.

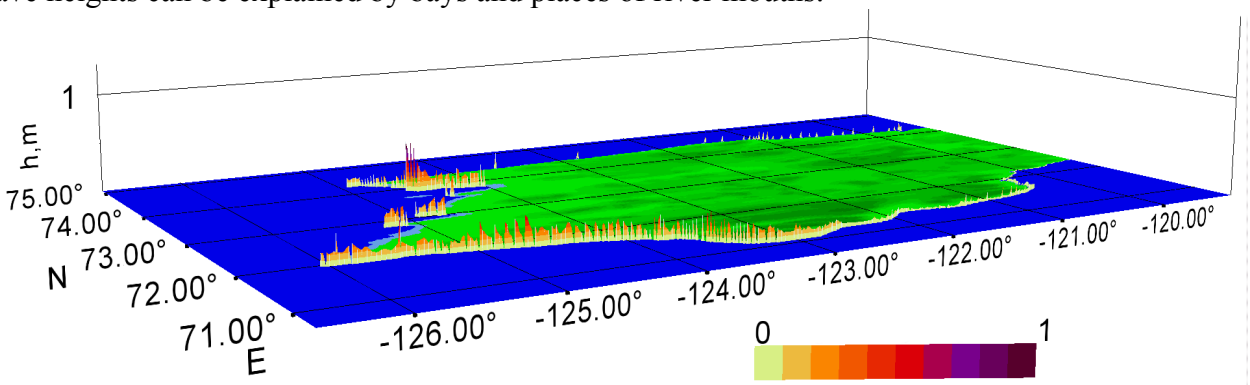

Fig. 17. 3D histogram of wave heights on Banks Island.

It should be noted that mainly on the coast, wave heights are minimal and do not exceed 10-15 centimeters. For a more detailed analysis of wave heights along the coast of the water area under consideration, data from virtual tide gauges (Table 7) were analyzed, which were placed near points along the coast of Canada. The wave with the largest amplitude came to the tide gauge located on the coast of Sachs Harbor.

Table 7. Data on maximum heights of wave displacement on the 5-meter isobath (according to tide gauge data) in the Beaufort Sea

Point	Max. height,m	Time, s
(1) Kendall Island Bird, Canada	**0,14**	**0:16:40**
(2) Paulatuk, Canada	**0,06**	**0:49:10**
(3) Sachs Harbour, Canada	**2,14**	**0:11:40**
(4) Ivvavik National Park, Canada	**0,90**	**0:25:25**
(5) Prudhoe Bay, USA	**0,15**	**0:40:25**

The wave started from a negative phase and went 0.6 meters relative to the water surface, after that the wave height rose to one meter and repeated about three times. The waves near the village of Paulatuk began with low tide, after which the height of the water surface rose by five centimeters. Ivvavik has a similar situation. The data captures the initial low tide, after which a uniform fluctuation of the water surface for two hours. In general, considering all tide gauge records one can conclude that all waves begin with a low tide and a sharp jump in wave heights of several tens of centimeters.

CONCLUSIONS

In this work, numerical simulation of possible tsunamis generated by seismic sources in the regions of historical earthquakes in the waters of the Arctic has been carried out. The strongest recorded earthquake in the Arctic Ocean basin was considered: in the Baffin Sea (1933) with a magnitude M = 7.7. 2 scenarios for each event were carried out within the framework of the keyboard model of the earthquake source, simulating different dynamics in the earthquake source. The results of numerical simulation were obtained in the work, in which the average height on the coast of Greenland lies in the range of 2-4m, and the maximum height of tsunami waves on the coast of the near zone of the source reaches 10-12m. In the Laptev Sea, 3 earthquakes with magnitudes 6.7 (1964), magnitude 6 (1923) and magnitude 5.5 (1969) were considered. A generalized earthquake source was built, which includes these 3 earthquakes with close localization. Estimates were made of the maximum wave heights for the mainland coast of Russia, where the population and infrastructure are most dense. The obtained wave characteristics were compared with the few available data of numerical simulations of these events by other authors. A comparison was made with the work of E.A. Kulikov et al., 2016, in which a certain difference was obtained, which, in our opinion, is associated with a more complex earthquake source model used in this work. In the Beaufort Sea, a simulation of the 1920 earthquake with a magnitude of 5.5 was carried out, an assessment of the wave fields was carried out according to

this water area, and results were also obtained on the maximum wave heights along part of the coast of Canada. It was found that the wave heights do not exceed 1.5m, which is in good agreement with the works of other authors. In contrast to the currently available, very limited number of works on the Arctic region, the work carried out a detailed tsunami zoning of the coasts of the three considered water areas within the Arctic basin.

ACKNOWLEDGEMENTS

The authors acknowledge the funding of this study provided by grant of President of the Russian Federation for the state support of Leading Scientific Schools of the Russian Federation (Grant No. NSH-70.2022.1.5.).

REFERENCES

1. ANSS ComCat. Composite Earthquake Catalog, Northern California Earthquake Data Center. 2014 // http://www.quake.geo.berkeley.edu/cnss/.

2. NGDC/WDS Global Historical Tsunami Database. doi:10.7289/V5PN93H7 // https:// www.ngdc.noaa.gov/ hazard/tsu_db.shtml.

4. Avetisov, G.P., 2004. Seismicity of the Arctic continental margin of Russia, Geol. T. 5: Arctic and Far Eastern seas. Book. 1: Arctic Seas / Ed. I. S. Gramberg, V. L. Ivanov, Yu. E. Pogrebitsky. SPb.: Publishing house of VSEGEI, 2004. S. 31-42.

5. Avetisov G. P., 1996. Seismically active zones of the Arctic. St. Petersburg: VNIIOkeanologiya, 1996. 186 p.

6. Mazur I.I., Ivanov O.P., 2004. Dangerous natural processes. Introductory course // M.: Economics, 2004. 702 p. ISBN 5-282-02406-3.

7. Kozelkov, A.S., Kurkin, A.A., Pelinovskii, E.N., Kurulin, V.V., 2015. Modeling the cosmogenic tsunami within the framework of the navier-stokes equations with sources of different types Fluid Dynamics, 2015, 50(2), pp. 306–313

8. E. A. Kulikov, A. I. Ivashchenko, I. P. Medvedev, O. I. Yakovenko, S. A. Kovachev, 2016. // Arctic: Ecology and Economics, No. 3 (23), 2016. P. 38 -49.

9. Phase et al., Kanao, S. Tsuboi, Rhett Butler, K. Anderson., 2016. Greenland Ice Sheet Dynamics and Glacial Earthquake Activities // BURRINO.19-T-12, 2013

10. Masaki Kanao, S. Tsuboi, Rhett Butler, K. Anderson, 2011. Greenland Ice Sheet Dynamics and Glacial Earthquake Activities // ROMBUNNO.15-T-15, 2011

11. Leonard L., Roger G., Mazotti S., 2014. Tsunami hazard assessment of Canada, Nat. Hazards. 2014. Vol. 70, No. 1. P. 237-274. DOI:10.1007/s11069-013-0809-5

12. The system of the Laptev Sea and the adjacent seas of the Arctic. 2009: the current state and history of development / Managing editors: X. Kassens, A.P. Lisitsyn, J. Tide, E.I. Polyakova, L.A. Timokhov, I.E. Frolov. - M.: Publishing House of Moscow. un-ta, 2009. 608 p.

13. Lobkovsky L.I., Baranov B.V. Keyboard, 1984. Model of strong earthquakes in island arcs and active continental margins // Doklady AN SSSR. T. 275. No. 4. S. 843-847. 1984.

14. Mazova R. Kh., Kurkin A. A, Giniyatullin A. R, Tyuntyayev C. M.. 2021. Earthquake of 30 October the Aegean Sea: Numerical Simulation of the Generation and Propagation of Tsunami Waves//(2021), V.40,N.3,pp.78-95

15. Wells D. L., Coppersmith K. J., 1994. New empirical relationships among magnitude, rupture length, rupture width, rupture area, and surface displacement // Bull. Seism. Soc. Am. 1994 Vol. 84. P. 974-1002.

16. Pelinovsky E.N., 1992. Nonlinear dynamics of tsunami waves. Gorky: Ed. IAP USSR Academy of Sciences. 1982. 226 p.

17. Voltsinger N.E., Klevanny K.A., Pelinovsky E.N., 1989. Long-wave dynamics of the coastal zone, Leningrad: Gidrometeoilzdat, 1989, 272 p.

18. Lobkovsky L.I., Baranov B.V., Mazova R.Kh., Kataeva L.Yu., 2006.Implications of the seismic source dynamics for the characteristics of a possible tsunami in a model problem of the seismic gap in the Central Kurile region // Russ. J. Earth Sci. 2006. V. 8. P. ES5002 (1–23). doi: 10.2205/2006ES000209 http://dx.doi.org/10.2205/2006ES000209

19. Lobkovsky, L.I. Garagash, B. Baranov, R. Mazova, N. Baranova, 2017. Modeling Features of Both the Rup ture Process and the Local Tsunami Wave Field from the 2011 Tohoku Earthquake // Pure Appl. Geophys. (2017). V.174, p. 3919-3938, doi:10.1007/s00024-017-1539-5 (March 2017) pp. 1-20.

20. Mazova R.Kh., Moiseenko T., Kurkin A.A., Jorge Van Den Bosch F., Gustavo Oses A., 2021 Numerical Simulation of a Catastrophic Earthquake and Strong Tsunami ofappril 1, 2014 near the Northwestern Part of the Chilian Coast// STH . (2021), , V.40, N.2, pp.83-100.

21. Sielecki, A., and M. Wurtele, 1970. The numerical integration of the nonlinear shallow water equations with sloping boundaries, J.Comput. Phys., 6, 219, 1970 doi: 10.1016/0021-9991(70)90022-7.